Cellular/Molecular

Reducing Agents Sensitize C-Type Nociceptors by Relieving High-Affinity Zinc Inhibition of T-Type Calcium Channels

Michael T. Nelson,[1,4] Jiwan Woo,[7] Ho-Won Kang,[5,6] Iuliia Vitko,[2] Paula Q. Barrett,[2] Edward Perez-Reyes,[2,4] Jung-Ha Lee,[5,6] Hee-Sup Shin,[7] and Slobodan M. Todorovic[1,3,4]

Departments of [1]Anesthesiology, [2]Pharmacology, and [3]Neuroscience and [4]Neuroscience Graduate Program, University of Virginia Health System, Charlottesville, Virginia 22908, [5]Department of Life Science and [6]Interdisciplinary Program of Biotechnology, Sogang University, Shinsu-Dong, Seoul 121-742, Korea, and [7]Center for Neural Science, Korea Institute of Science and Technology, Hawolgok-Dong, Seongbuk-Gu, Seoul 136-791, Korea

Recent studies have demonstrated an important role for T-type Ca^{2+} channels (T-channels) in controlling the excitability of peripheral pain-sensing neurons (nociceptors). However, the molecular mechanisms underlying the functions of T-channels in nociceptors are poorly understood. Here, we demonstrate that reducing agents as well as endogenous metal chelators sensitize C-type dorsal root ganglion nociceptors by chelating Zn^{2+} ions off specific extracellular histidine residues on $Ca_v3.2$ T-channels, thus relieving tonic channel inhibition, enhancing $Ca_v3.2$ currents, and lowering the threshold for nociceptor excitability *in vitro* and *in vivo*. Collectively, these findings describe a novel mechanism of nociceptor sensitization and firmly establish reducing agents, as well as Zn^{2+}, Zn^{2+}-chelating amino acids, and Zn^{2+}-chelating proteins as endogenous modulators of $Ca_v3.2$ and nociceptor excitability.

Key words: **dorsal root ganglion; action potential; C-fiber; calcium current; nociception; pain; sensitization; zinc**

Introduction

After injury, peripheral pain-sensing neurons (nociceptors) can become hyperexcitable, or "sensitized." Electrophysiologically, peripheral sensitization is manifest as lower thresholds for neuronal activation and higher frequencies of action potentials (APs) that are either spontaneous or evoked by suprathreshold stimuli (Bhave and Gereau, 2004). Although initially protective, peripheral sensitization can lead to long-term changes in spinal sensory pathways and chronic pain hypersensitivity (central sensitization) that outlasts any physiological function (Campbell and Meyer, 2006). Sensitization is a characteristic of many pain conditions, but the mechanisms underlying its initiation and maintenance are poorly understood.

We reported previously that reducing agents such as dithiothreitol (DTT) and L-cysteine (L-cys) selectively enhance T-type Ca^{2+} currents (T-currents) in dorsal root ganglion (DRG) nociceptors *in vitro* and produce thermal and mechanical sensitization when injected into the peripheral receptive fields of these neurons *in vivo* (Todorovic et al., 2001). Furthermore, reducing agents sensitize a unique subpopulation of DRG nociceptors, termed "T-rich" cells (Nelson et al., 2005). Among small DRG cells, T-rich cells display an unusually high density of T-currents and a low density of high-voltage-activated (HVA) Ca^{2+} currents. However, T-rich cells are atypical nociceptors and are distinct from the majority of classically described, presumably C-type, DRG nociceptors that express large HVA currents and moderate T-currents (Scroggs and Fox, 1992; Cardenas et al., 1995), as well as the minority subpopulation of C-type cells that lack T-currents altogether (Cardenas et al., 1995).

Here, we show that reducing agents selectively sensitize C-type nociceptors that express $Ca_v3.2$ T-currents. We then demonstrate that the sensitization is facilitated through a novel mechanism, whereby reducing agents chelate Zn^{2+} ions off specific extracellular histidine residues in domain I of $Ca_v3.2$, thereby relieving tonic channel inhibition. Last, we show that reducing agents, as well as synthetic and endogenous Zn^{2+} chelators, sensitize $Ca_v3.2$ current-containing C-type nociceptors from wild-type mice but not C-type nociceptors from $Ca_v3.2^{-/-}$ mice *in vitro* and *in vivo*. Collectively, our data further support a role for $Ca_v3.2$ channels in peripheral nociception and identify a novel mechanism for $Ca_v3.2$ modulation that underlies nociceptor sensitization.

Materials and Methods

DRG neurons. Acutely dissociated DRG cells were prepared from adolescent Sprague Dawley rats, adult C57BL/6J mice, or adult $Ca_v3.2^{-/-}$ mice (Chen et al., 2003) as described previously (Nelson et al., 2005). For recordings, cells were plated onto uncoated glass coverslips, placed in a culture dish, and perfused with external solution. All experiments were performed at room temperature.

HEK293 cells. HEK293 cells were grown in DMEM/F-12 media (Invitrogen, Grand Island, NY) supplemented with fetal calf serum (10%), penicillin G (100 U/ml), and streptomycin (0.1 mg/ml). $Ca_v3.1$ (Perez-Reyes et al., 1998), $Ca_v3.2$ (Vitko et al., 2005), and GGHH (Welsby et al., 2003) plasmids were as described. HHGG, GHGG, HGGG, $Ca_v3.2$(H191Q), and $Ca_v3.1$(Q172H) plasmids were constructed as de-

Received April 20, 2007; revised June 19, 2007; accepted June 20, 2007.

This work was supported by National Institutes of Health Grants NS054521 (M.T.N.), GM075299 (S.M.T.), NS38691 (E.P.-R.), and HL36977 (P.Q.B.), as well a grant from the Korean National Honor Scientist Program (H.-S.S.). We thank Dr. Kevin Campbell of the University of Iowa for the initial breeding pair of $Ca_v3.2^{-/-}$ mice and Le Banh of the University of Virginia for helpful comments on this manuscript.

Correspondence should be addressed to Slobodan M. Todorovic, Department of Anesthesiology, University of Virginia Health System, Box 800710, Charlottesville, VA 22908. E-mail: st9d@virginia.edu.

DOI:10.1523/JNEUROSCI.1800-07.2007

 0270-6474/07/278250-11$15.00/0

scribed previously (Kang et al., 2006) and subcloned into pcDNA3 (Invitrogen). Cells were cotransfected using Lipofectamine 2000 (Invitrogen) at a 10:1 molar ratio with a plasmid encoding CD8 antigen and incubated with polystyrene microbeads coated with anti-CD8 antibody (Invitrogen). After 48 h, cells with bound microbeads were selected for recording.

Electrophysiology. Recording electrodes pulled from borosilicate glass microcapillary tubes (Drummond Scientific, Broomall, PA) had resistances from 1–4 MΩ when filled with internal solution. Recordings were made using an Axopatch 200B patch-clamp amplifier (Molecular Devices, Foster City, CA). Digitization of membrane voltages and currents were controlled using a Digidata 1322A interfaced with Clampex 8.2 (Molecular Devices). We analyzed data using Clampfit 8.2 (Molecular Devices) and Origin 7.0 (Microcal Software, Northampton, MA). Currents were low-pass filtered at 2–5 kHz. Series resistance and capacitance values were taken directly from readings of the amplifier after electronic subtraction of the capacitive transients. Series resistance was compensated to the maximum extent possible (usually 50–80%). In some experiments, a P/5 protocol was used for on-line leak subtractions. Multiple independently controlled glass syringes served as reservoirs for a gravity-driven perfusion system. Solution exchange was accomplished by constant suction through a glass capillary tube at the opposite end of the recording dish. The external solution used for current-clamp recordings contained the following (in mM): 140 NaCl, 10 glucose, 10 HEPES, 4 KCl, 2 $CaCl_2$, and 2 $MgCl_2$, adjusted to pH 7.4. The external solution used for voltage-clamp recordings contained the following (in mM): 152 tetraethylammonium (TEA)-Cl, 10 $BaCl_2$, and 10 HEPES, adjusted to pH 7.4 with TEA-OH. The internal solution used for current-clamp recordings contained the following (in mM): 130 KCl, 40 HEPES, 5 $MgCl_2$, 2 Mg-ATP, 1 EGTA, and 0.1 Na-GTP, adjusted to pH 7.2 with KOH. The internal solution used for voltage-clamp recordings contained the following (in mM): 110 Cs-$MeSO_4$, 14 Cr-PO_4, 10 HEPES, 9 EGTA, 5 Mg-ATP, and 0.3 Tris-GTP, adjusted to pH 7.3 with CsOH. All drugs were prepared as stocks and freshly diluted at the time of experiments. Bovine serum albumin (BSA), DTT, L-cys, L-histidine (L-his), tricine, and Zn^{2+} were dissolved in H_2O; cuprizone, 5,5′dithio-bis-2-nitrobenzoic acid (DTNB), mibefradil, and N-ethylmaleimide (NEM) were dissolved in DMSO; diethylenetriaminepentaacetic acid (DTPA) and EDTA were dissolved in 1 M NaOH, adjusted to pH 7.4; and *N*,*N*,*N*′,*N*′-tetra-2-picolylethylenediamine (TPEN) was dissolved in 0.1 M HCl. Short pulses (1 s) of broad-spectrum ultraviolet (UV) light (Double Bore UV lamp; Jelight Company, Irvine, CA) were applied to cells at a distance of 1 cm.

Buffered Zn^{2+} solutions. The apparent high affinity of $Ca_v3.2$ channels for Zn^{2+} and the substantial tonic inhibition of these channels by contaminating Zn^{2+} in our recording solutions necessitated the use of buffered Zn^{2+} solutions to establish an accurate concentration–response relationship (see Fig. 5). For these experiments, calibrated free Zn^{2+} concentrations were obtained using the low-affinity Zn^{2+} chelator tricine (K_D of 10–5 M), according to the empirically determined method of Paoletti et al. (1997). Nominally "Zn^{2+}-free" reference solutions were made by substituting 10 mM tricine for 10 mM HEPES in our normal external solution with no additional Zn^{2+}.

Behavioral studies. $Ca_v3.2^{-/-}$ mice were generated as described previously (Chen et al., 2003). The *$Ca_v3.2^{-/-}$* mutation was maintained in two different inbred backgrounds (129s4/SvJae and C57BL/6J) by repeated back-crossing into each genetic background for >10 generations. The hybrid F1 *$Ca_v3.2^{-/-}$* and wild-type littermate control mice were generated by mating heterozygotes from the two genetic backgrounds (129s4/SvJae.$Ca_v3.2^{+/-}$ and C57BL/65J.$Ca_v3.2^{+/-}$). Mice were maintained with access to food and water ad libitum in a 12 h light/dark cycle. Animal care and handling were according to the guidelines of the Institutional Animal Care and Use Committee of the Korea Institute of Science and Technology. Hindpaw thermal sensitivity was assessed using a Hargreaves test (Hargreaves et al., 1988; Jevtovic-Todorovic et al., 1998) conducted with a plantar test device (7371 plantar test; Ugo Basile, Comerio, Italy). Animals were allowed to freely move within an open-top, glass-bottom, transparent plastic chamber (9 cm square, 14 cm tall). Mice were accommodated for 60 min before testing. A mobile radiant heat source was placed under the glass floor and focused onto the left paw. Paw-withdrawal latencies (PWLs) were measured with a cutoff time of 15 s. To test the effects of L-cys, we injected 10 μl intradermally in the ventral side of the left hindpaw. Wild-type littermates were used as a control.

Analysis. For electrophysiological experiments, statistical comparisons were made using paired or unpaired *t* tests or Mann–Whitney *U* tests when appropriate. For behavioral experiments, statistical comparisons were made using two-way repeated-measure ANOVAs. All data are expressed as mean ± SEM, and *p* values are reported only when statistically significant (<0.05). The voltage dependencies of activation and steady-state inactivation were described with single Boltzmann distributions of the following forms:

$$G(V) = G_{max}/(1 + exp[-(V - V_{50})/k]) \quad (1)$$

$$I(V) = I_{max}/(1 + exp[(V - V_{50})/k]), \quad (2)$$

where G_{max} is the maximal conductance, I_{max} is the maximal activatable current, V_{50} is the voltage in which half of the current is activated or inactivated, and k represents the voltage dependence (slope) of the distribution. The percentage reductions in peak current at various Zn^{2+} concentrations were used to generate concentration–response curves. Mean values were fit to the following Hill–Langmuir function:

$$PB([Zn^{2+}]) = PB_{max}/(1+(IC_{50}/[Zn^{2+}])^h), \quad (3)$$

where PB_{max} is the maximal percentage inhibition of peak current, IC_{50} is the concentration that produces 50% inhibition, and h is the apparent Hill–Langmuir coefficient for inhibition. The fitted values are reported with >95% linear confidence limits.

Results

L-cys sensitizes T-current-containing rat C-type DRG nociceptors

APs were recorded from 10 small, acutely dissociated, rat DRG neurons (diameter of 26.0 ± 0.5 μm). Cells had an average resting membrane potential (RMP) of −63 ± 1 mV. We used short current injections (1 ms) to avoid contamination of the AP waveform with that of the stimulus. APs had long durations (13 ± 3 ms at base), positive peaks (46 ± 3 mV), and long-lasting after-hyperpolarizations (AHPs) (all cells >75 ms) (Fig. 1*A*,*E*), properties that are characteristic of C-type nociceptors (Harper and Lawson, 1985; Petruska et al., 2000; Fang et al., 2005). To assess the effects of reducing agents on T-current-dependent excitability, cells were manually hyperpolarized to membrane potentials ranging from −80 to −95 mV to maximize the availability of T-channels for activation (Nelson et al., 2005). Using increasingly stronger current injections (Δ100 pA), we determined the threshold current necessary to evoke an overshooting AP in each cell in the presence and absence of L-cys. In 7 of 10 cells, L-cys lowered the threshold for excitability (responders). Among these cells, threshold was decreased by an average of 200 pA in the presence of L-cys (control, 1.9 ± 0.2 nA; L-cys, 1.7 ± 0.2 nA; $p < 0.05$) (Fig. 1*B*). In contrast, in three cells (nonresponders), the threshold was unchanged by L-cys (Fig. 1*F*). Moreover, in responders, L-cys doubled the probability of AP firing elicited by trains of subthreshold current injections (control, 34 ± 4%; L-cys, 68 ± 7%; $p < 0.01$) (Fig. 1*C*). L-cys did not affect passive membrane properties such as membrane potential or input resistance (R_i) in responsive or nonresponsive cells (R_i control, 1.5 ± 0.3 GΩ; R_i L-cys, 1.5 ± 0.2 GΩ).

Because L-cys selectively increases T-currents over other voltage- and ligand-gated currents in DRG nociceptors (Todorovic et al., 2001), we reasoned that L-cys-induced sensitization should only occur in C-type cells expressing T-currents. Thus, whenever possible, after current-clamp recording, current–voltage (*I*–*V*) data were obtained for each cell under voltage-clamp in

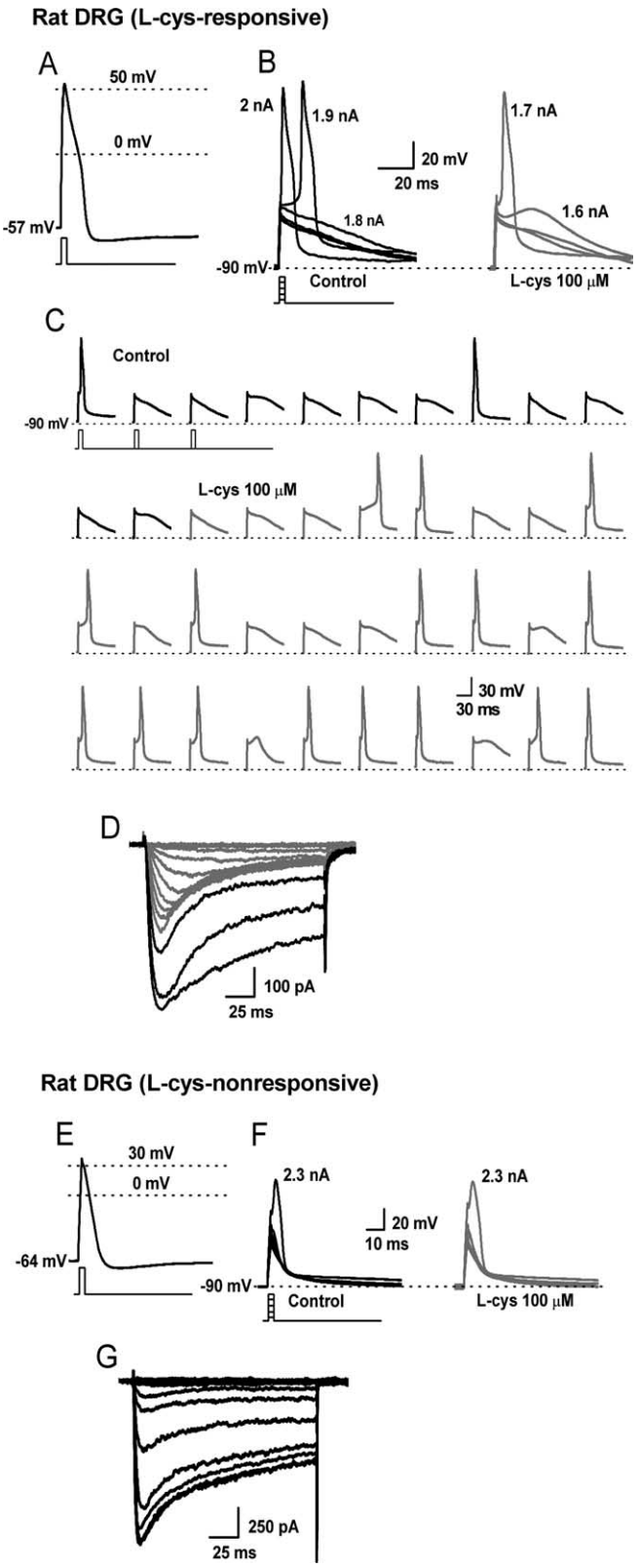

Figure 1. The effects of L-cys on the excitability of T-current-containing and T-current-deficient rat C-type nociceptors. ***A–D***, Traces are from a single, acutely dissociated, L-cys-sensitive rat DRG neuron. ***E–G***, Traces from another, acutely dissociated, L-cys-insensitive rat DRG neuron. ***A***, AP elicited by a 1 ms, 2 nA current injection at the RMP of the cell. ***B***, The cell was manually hyperpolarized to −90 mV and progressively greater current injections (Δ100 pA) delivered every 10 s to determine the threshold for AP firing. Threshold was 1.9 nA in control (left) and 1.7 nA in the presence of L-cys (right). ***C***, Continuous segment of an experiment showing that L-cys increases the probability (percentage) to fire APs in response to trains of subthreshold stimuli (stimuli were 1 ms, 1.7 nA delivered every 10 s). ***D***, *I–V* traces recorded in Ca^{2+} current-isolating external solution after current-clamp recording. Note the presence of both T-type (rapidly inactivating; gray lines) and HVA (slowly inactivating; black lines) currents. ***E***, AP elicited by a 1 ms, 2.5 nA current injection at the RMP of the cell. ***F***, Threshold was unaffected by the application of L-cys. ***G***, *I–V* traces; note the presence of only HVA currents.

Ca^{2+} current-isolating external solution. Among the seven responders, five survived the perfusion-configuration exchange, and, in each cell, both T-type and HVA currents were observed (Fig. 1*D*). In contrast, all nonresponders survived, and in every cell we detected only HVA currents (Fig. 1*G*).

H191 is required for the reducing agent sensitivity of $Ca_v3.2$ T-channels

We reported previously that reducing agents enhance $Ca_v3.2$ T-currents but not $Ca_v3.1$ or $Ca_v3.3$ T-currents, whereas oxidizing agents such as DTNB inhibit all three T-currents to a similar degree (Joksovic et al., 2006). Furthermore, knock-out studies have demonstrated that $Ca_v3.2$ is overwhelmingly the predominant T-channel isoform in small DRG neurons (Chen et al., 2003). Thus, to identify the molecular site of action of reducing agents on T-channels in C-type nociceptors, we screened the DTT and L-cys sensitivity of a series of chimeric channels constructed between $Ca_v3.1$ (α1G) and $Ca_v3.2$ (α1H) expressed in HEK293 cells. The chimeras were named using letters to represent the α-subunit donor for each of the four channel domains (Fig. 2). Between two half-channel chimeras, GGHH currents were insensitive to DTT and L-cys, whereas HHGG currents were sensitive to both, suggesting that domains I and/or II of $Ca_v3.2$ were possible sites of reducing agent modulation (Fig. 2*A*,*B*). Based on these findings, we screened two single-domain chimeras, swapping either domain I or II between channel isoforms. GHGG currents were insensitive to DTT and L-cys, whereas HGGG currents were sensitive, thereby identifying domain I of $Ca_v3.2$ as a critical determinant of reducing agent action (Fig. 2*C*,*D*). Because the effects of oxidizing agents are conserved across T-channels (Joksovic et al., 2006), we were unable to track their molecular determinant using this chimeric strategy.

Interestingly, the sensitivity of the chimeras to reducing agents mimics their previously reported inhibition by Ni^{2+}. This is of interest because, similar to reducing agents, Ni^{2+} is one of the few agents capable of discriminating among T-channel isoforms, because $Ca_v3.2$ is ~20-fold more sensitive than $Ca_v3.1$ or $Ca_v3.3$ (Lee et al., 1999; Jeong et al., 2003). Furthermore, mutation of a single extracellular histidine (H) residue to glutamine (Q) at position 191 (H191Q) was shown to greatly diminish the Ni^{2+} sensitivity of $Ca_v3.2$ (Kang et al., 2006). Based on these observations and studies demonstrating that thiol-containing reducing agents are excellent metal chelators (Krezel et al., 2001), we screened the sensitivity of $Ca_v3.2$(H191Q) to DTT and L-cys. Similar to our previous report on stably expressed channels (Joksovic et al., 2006), both DTT and L-cys significantly increased currents from transiently expressed $Ca_v3.2$ (Fig. 3*A*,*B*). Conversely, the effects of DTT and L-cys were completely abolished in $Ca_v3.2$(H191Q) (Fig. 3*C*,*D*). These results are consistent with our previous recordings from cell-free patches, which predicted that the critical determinants for reducing agent modulation would be located on the extracellular side of $Ca_v3.2$ (Joksovic et al., 2006). We next compared the electrophysiological profiles of $Ca_v3.2$ to $Ca_v3.2$(H191Q) in the presence and absence of DTT. DTT increased $Ca_v3.2$ currents over the entire *I–V* range and shifted the

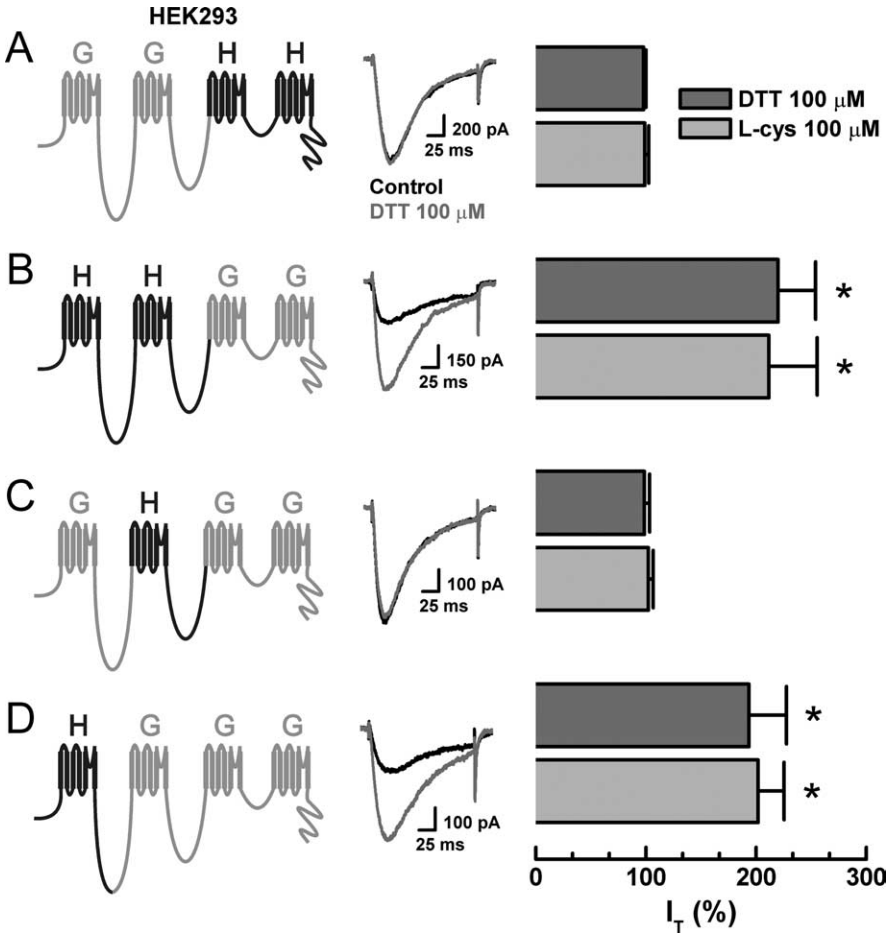

Figure 2. Reducing agent sensitivity of serial chimeras constructed from $Ca_v3.1$ (α1G) and $Ca_v3.2$ (α1H) T-channels. Currents were evoked from HEK293 cells expressing the indicated constructs by steps from −90 to −30 mV, before and during exposure to DTT. Histograms display averaged effects of DTT and L-cys in each construct expressed as percentage of control ($n = 5–9$). ***A***, GGHH: DTT, 98 ± 2%; L-cys, 99 ± 4%. ***B***, HHGG: DTT, 220 ± 34%, *$p < 0.01$; L-cys, 211 ± 44%, $p < 0.01$. ***C***, GHGG: DTT, 99 ± 5%; L-cys, 102 ± 4%. ***D***, HGGG: DTT, 193 ± 34%, *$p < 0.01$; L-cys, 202 ± 24%, $p < 0.01$.

voltage dependence of activation 5 mV to the left but had little effect on steady-state inactivation (Fig. 3*E–G*). The biophysical parameters of $Ca_v3.2$(H191Q) currents were very similar to $Ca_v3.2$ currents but were not modulated by DTT (Fig. 3*H–J*). We next attempted to confer reducing agent sensitivity to $Ca_v3.1$ by performing the analogous reverse mutation (Q172H). $Ca_v3.1$(Q172H) currents were significantly enhanced by DTT and L-cys (Fig. 3*K*). Additionally, inhibition by the nonselective T-channel antagonist mibefradil was unaffected by either point mutation (Fig. 3*L*).

Metal chelators mimic and occlude the effects of reducing agents

Previous studies have demonstrated that two major mechanisms generally underlie modulation of ion channels by DTT and L-cys: reduction of cysteine residues (Sullivan et al., 1994; Choi et al., 2001) and chelation of metal ions bound to residues such as aspartate, cysteine, glutamate, and histidine (Choi and Lipton, 1999; Fayyazuddin et al., 2000; Wilkins and Smart, 2002; Chu et al., 2004). Because H191 is critical for both the effects of reducing agents and metal binding to $Ca_v3.2$, we conducted experiments to determine whether the modulation by DTT and L-cys could be attributed to chelation of a metal bound at this site. Application of the nonselective, membrane-impermeable chelator DTPA enhanced $Ca_v3.2$ currents to a similar degree as DTT and L-cys (Fig. 4*A*,*C*) but had no effect on $Ca_v3.2$(H191Q) or $Ca_v3.1$ currents (Fig. 4*C*). Furthermore, DTPA occluded the effects of subsequently applied L-cys (Fig. 4*B*). Application of EDTA, another nonselective, membrane-impermeable chelator, mimicked the effects of DTPA (Fig. 4*D*). To identify the specific metal bound, we used a variety of chelators with more selective metal affinities. Anecdotally, the metal was unlikely to be Ca^{2+} or Ba^{2+} because, in our experiments, DTPA, DTT, EDTA, and L-cys all greatly enhanced T-currents at concentrations of 100 μM or less despite the presence of 2 mM Ca^{2+} (current-clamp) or 10 mM Ba^{2+} (voltage-clamp) as the charge carrier. Because histidine residues have a particularly high affinity for divalent transition metals such as Cu^{2+}, Ni^{2+}, and Zn^{2+} (Sundberg and Martin, 1974), we considered these particularly likely candidates.

Interestingly, Zn^{2+} is the most prevalent trace metal contaminant of common electrophysiological solutions (Li et al., 1996; Paoletti et al., 1997; Thio and Zhang, 2006), and its chelation is sufficient to remove a substantial degree of tonic inhibition from highly Zn^{2+}-sensitive ion channels such as NR1/NR2A NMDA receptors (Paoletti et al., 1997). Consistent with this idea, the application of TPEN, a potent Zn^{2+} chelator with much lower affinity for Ba^{2+}, Ca^{2+}, and Mg^{2+}, dramatically increased $Ca_v3.2$ currents (Fig. 4*D*). Correspondingly, application of the low-affinity but relatively Zn^{2+}-selective chelator tricine also greatly increased $Ca_v3.2$ currents, whereas the relatively Cu^{2+}-selective chelator cuprizone effected a smaller, but significant, current increase (Fig. 4*D*,*E*). These data suggest that, in our system, $Ca_v3.2$ currents are subject to tonic inhibition by a variety of trace metal ions, with Zn^{2+} predominating. Furthermore, the enhancement of these currents by DTT and L-cys is likely attributable to the ability of these agents to act as metal chelators.

Zn^{2+} is present at high levels *in vivo* but, because of toxicity in its free form, is almost always protein bound in the body. For example, in blood, ~69% of Zn^{2+} is transported with albumin, ~30% with α_2-macroglobulin, and ~1% with cysteine and histidine (Richelle et al., 2006). Consistent with this idea, both BSA and L-his significantly increased $Ca_v3.2$ currents (Fig. 4*F–J*) at physiologically relevant concentrations (Iresjo et al., 2006). Similar to DTPA, BSA had no effect on $Ca_v3.2$(H191Q) or $Ca_v3.1$ currents and occluded the effects of L-cys (Fig. 4*G*).

Mutation of H191 disrupts high-affinity Zn^{2+} inhibition of $Ca_v3.2$

As mentioned previously, the Ni^{2+} sensitivity of $Ca_v3.2$ is dramatically reduced by the H191Q mutation (Kang et al., 2006). However, our data suggests that the tonic inhibition of $Ca_v3.2$ in our system is primarily attributable to Zn^{2+}. Thus, we wanted to determine whether Zn^{2+} binding was also abnormal in

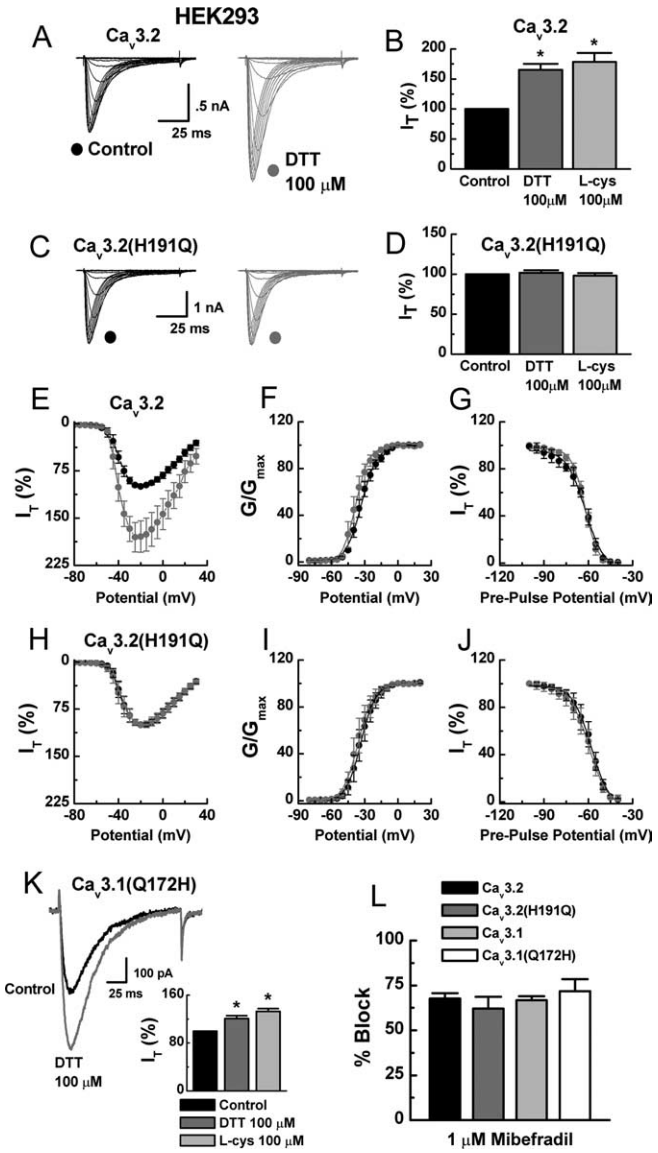

Figure 3. H191 is required for the reducing agent sensitivity of $Ca_v3.2$. ***A***, Currents evoked from HEK293 cells expressing $Ca_v3.2$ by steps from −90 to 0 mV (Δ5 mV), before and during exposure to DTT. ***B***, Averaged effects of DTT and L-cys on $Ca_v3.2$ currents expressed as percentage of control: DTT, 165 ± 10%, $n = 32$, $^*p < 0.01$; L-cys, 178 ± 15%, $n = 17$, $^*p < 0.01$. ***C***, Currents evoked from HEK293 cells expressing $Ca_v3.2$(H191Q), before and during exposure to DTT. ***D***, Averaged effects of DTT and L-cys on $Ca_v3.2$(H191Q) currents expressed as percentage of control: DTT, 102 ± 3%, $n = 15$; L-cys, 98 ± 3%, $n = 11$. ***E***, Averaged effects of DTT on $Ca_v3.2$ currents evoked by steps from −90 to −80 through 30 mV ($n = 7$). ***F***, Effects of DTT on voltage-dependent activation of $Ca_v3.2$ currents calculated from *I–V* data and fit with Equation 1: control, V_{50} of −33.0 ± 0.3 mV, $k = 7.0 \pm 0.3$; DTT, V_{50} of −38.0 ± 0.4 mV, $k = 6.0 \pm 0.3$. ***G***, Effects of DTT on steady-state inactivation of $Ca_v3.2$ currents. Currents were recorded at −30 mV after 3.5-s-long prepulses to potentials ranging from −100 to −40 mV. Averaged data were fit with Equation 2: control, V_{50} of −62.0 ± 0.6 mV, $k = 6.0 \pm 0.6$; DTT, V_{50} of −62.0 ± 0.4 mV, $k = 5.0 \pm 0.4$; $n = 6$. ***H***, Averaged effects of DTT on $Ca_v3.2$(H191Q) currents evoked by steps from −90 to −80 through 30 mV ($n = 6$). ***I***, Effects of DTT on voltage-dependent activation of $Ca_v3.2$(H191Q) currents: control, V_{50} of −34.0 ± 0.4 mV, $k = 6.0 \pm 0.2$; DTT, V_{50} of −35.0 ± 0.4 mV, $k = 7.0 \pm 0.3$. ***J***, Effects of DTT on steady-state inactivation of $Ca_v3.2$(H191Q) currents: control, V_{50} of −58.0 ± 0.6 mV, $k = 6.0 \pm 0.4$; DTT, V_{50} of −60.0 ± 0.6 mV, $k = 6.0 \pm 0.4$; $n = 6$. ***K***, Raw traces and averaged effects of DTT and L-cys on $Ca_v3.1$(Q172H) currents expressed as percentage of control: DTT, 121 ± 5%, $n = 11$, $^*p < 0.01$; L-cys, 132 ± 5%, $n = 5$, $^*p < 0.01$. ***L***, Mibefradil inhibition of currents evoked from the indicated constructs expressed as percentage of control: $Ca_v3.2$, 68 ± 4%; $Ca_v3.2$(H191Q), 62 ± 7%; $Ca_v3.1$, 67 ± 2%; $Ca_v3.1$(Q172H), 71 ± 7%; $n = 5–6$.

$Ca_v3.2$(H191Q). A previous study reported an IC_{50} value for Zn^{2+} inhibition of $Ca_v3.2$ of 2.3 μM under nearly identical recording conditions (Jeong et al., 2003). However, this study did not take into account the possible presence of contaminating Zn^{2+} in the recording solutions, and the solutions with no added Zn^{2+} were assumed to be Zn^{2+} free. This prompted us to reevaluate the concentration–response relationship of Zn^{2+} and $Ca_v3.2$ using a tricine buffering system, which allows for creation of nominally Zn^{2+} free reference solutions as well as control of free Zn^{2+} concentrations (see Materials and Methods). As shown in Figure 5, the apparent IC_{50} for Zn^{2+} inhibition of $Ca_v3.2$ using tricine-buffered solutions was 890 nM. This apparent increase in sensitivity was expected because removal of baseline inhibition by Zn^{2+} contaminates would be predicted to unmask a portion of previously hidden sensitivity. Previous studies on other highly Zn^{2+}-sensitive ion channels such as NR1/NR2A NMDA receptors (Paoletti et al., 1997) and acid-sensing ion channels (ASICs) (Chu et al., 2004) have reported similar findings, in which the apparent IC_{50} value for Zn^{2+} inhibition was reduced using tricine. Interestingly, Traboulsie et al. (2007) found the IC_{50} for Zn^{2+} inhibition of $Ca_v3.2$ in HEK293 cells to be nearly identical (800 nM) but without tricine, which likely suggests that their solutions are minimally contaminated with Zn^{2+}, or may be attributable to differences in the charge carrier used (2 mM Ca^{2+} vs 10 mM Ba^{2+}), which can also affect concentration–response relationships. In contrast, $Ca_v3.2$(H191Q) was unaffected by chelators and had an apparent IC_{50} for Zn^{2+} inhibition of 42 μM (Fig. 5). Collectively, these data suggest that $Ca_v3.2$ channels are highly Zn^{2+} sensitive, and that the H191Q mutation dramatically reduces this sensitivity.

Cysteine-modifying agents do not prevent the effects of reducing agents

Previous studies have demonstrated that, in several redox-sensitive ion channels, modulation by reducing agents involves both chelation of Zn^{2+} from high-affinity binding sites, as well as reduction of cysteine residues, as evidenced by mutational studies, and the fact that Zn^{2+} chelators do not completely occlude the effects of subsequently applied reducing agents (Pan et al., 2000; Choi et al., 2001; Wilkins and Smart, 2002; Chu et al., 2006). However, our mutation and occlusion experiments suggest that reduction of cysteine residues contributes very little to the effects of reducing agents on $Ca_v3.2$. Furthermore, all extracellular cysteine residues in domain I of $Ca_v3.2$ are conserved across T-channels, and the effects of DTT and L-cys are readily reversible, even when applied at millimolar concentrations for many minutes (data not shown). These observations are inconsistent with traditional cysteine reduction, which generally requires millimolar concentrations of reducing agents and is essentially irreversible during washout of the agent (Choi et al., 2001; Wilkins and Smart, 2002). Nonetheless, to further rule out involvement of cysteine reduction in the modulation of $Ca_v3.2$ by reducing agents, we attempted to disrupt the effects of these agents using various cysteine modifiers. Application of the irreversible thiol-alkylator NEM did not prevent subsequent enhancement of $Ca_v3.2$ currents by DTT (Fig. 6*A*) but significantly attenuated their inhibition by DTNB (Fig. 6*B*), suggesting that the effects of oxidizing but not reducing agents depend on modification of conserved cysteine residues. However, experiments with NEM are inherently problematic because the concentrations and application durations required for complete thiol alkylation vary greatly from channel to channel and can be inhibited for steric, pH, or charge-related reasons. Thus, results, particularly

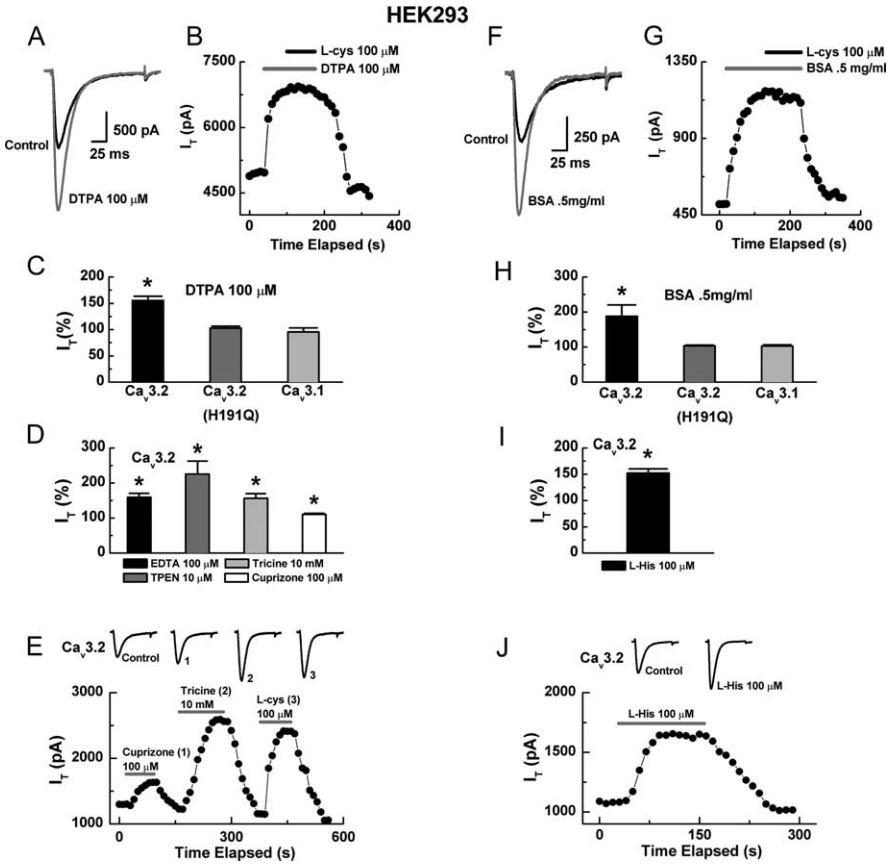

Figure 4. Synthetic and endogenous metal chelators mimic and occlude the effects of reducing agents. ***A***, Currents evoked from HEK293 cells expressing $Ca_v3.2$ by steps from −90 to −30 mV, before and during exposure to DTPA. ***B***, Time course showing that application of DTPA occludes the effect of subsequently applied L-cys; similar results were obtained in four additional cells. ***C***, Averaged effects of DTPA on currents from the indicated constructs expressed as percentage of control: $Ca_v3.2$, 155 ± 8%, $n = 5$, $^*p < 0.01$; $Ca_v3.2$(H191Q), 107 ± 4%, $n = 6$; $Ca_v3.1$ 95 ± 8%, $n = 5$. ***D***, Averaged effects of various chelators on $Ca_v3.2$ currents expressed as percentage of control: EDTA, 159 ± 11%; TPEN, 225 ± 37%; tricine, 156 ± 14%; cuprizone, 111 ± 3%; $n = 6–8$, $^*p < 0.01$. ***E***, Time course and raw traces comparing the effects of cuprizone, tricine, and L-cys on $Ca_v3.2$ currents. ***F***, Currents evoked from $Ca_v3.2$ before and during exposure to BSA. ***G***, Time course showing that application of BSA occludes the effect of subsequently applied L-cys. ***H***, Averaged effects of BSA on currents from the indicated constructs expressed as percentage of control: $Ca_v3.2$, 188 ± 32%, $n = 4$, $^*p < 0.01$; $Ca_v3.2$(H191Q), 103 ± 3%, $n = 5$; $Ca_v3.1$, 103 ± 4%, $n = 5$. ***I***, Averaged effects of L-his on $Ca_v3.2$ currents expressed as percentage of control: 152 ± 8%, $n = 6$, $^*p < 0.01$. ***J***, Time course and raw traces showing the effects of L-his on $Ca_v3.2$ currents.

negative results, with NEM must be interpreted with caution. However, we found that the same concentration and application duration of NEM that failed to inhibit the effects of DTT on $Ca_v3.2$ prevented the enhancement of GABA currents in DRG neurons by DTT ($n = 5$; data not shown), a modulation shown previously to involve reduction of cysteine residues (Pan et al., 2000). These data serve as a positive control and further suggest that cysteine reduction does not significantly contribute to reducing agent modulation of $Ca_v3.2$.

To further rule out reduction of cysteine residues as a mechanism by which reducing agents modulate $Ca_v3.2$ channels, we delivered brief pulses (1 s) of UV light to disrupt putative disulfide bonds. In several redox-sensitive ion channels, this treatment has been shown to mimic the effects of DTT as well as to prevent modulation by subsequent applications of DTT (Leszkiewicz and Aizenman, 2002, 2003). In our system, UV light had no independent effect on $Ca_v3.2$ currents and did not occlude the effects of DTT (Fig. 6*C*), again indicating that reduction of cross-linked cysteine residues does not contribute significantly to DTT modulation of $Ca_v3.2$.

Reducing agents and chelators sensitize C-type DRG nociceptors from wild-type but not $Ca_v3.2^{-/-}$ mice *in vitro* and *in vivo*

Based on our molecular findings, we examined whether reducing agents and chelators could sensitize C-type nociceptors isolated from wild-type mice as well as $Ca_v3.2^{-/-}$ mice, which express no T-currents in their DRG neurons (Chen et al., 2003). APs were recorded from nine small, acutely dissociated wild-type neurons. Cells had an average diameter of 26.0 ± 0.4 μm and RMPs of −58 ± 4 mV. APs had long durations (8 ± 1 ms), positive peaks (38 ± 3 mV), and long-lasting AHPs (all cells >75 ms), again consistent with identification as C-type nociceptors (Fig. 7*A*). In seven wild-type cells, BSA lowered the threshold for excitability, whereas two cells did not respond. Among responders, AP threshold was lowered 150 pA in the presence of BSA (control, 1.88 ± 0.09 nA; BSA, 1.73 ± 0.07 nA; $p < 0.05$) (Fig. 7*C*). BSA also greatly increased the probability of AP firing elicited by trains of subthreshold current injections, as did L-cys, DTPA, and TPEN (Fig. 7*C*,*E*). Threshold and subthreshold firing probability were both unchanged in the two nonresponsive cells (data not shown). BSA did not affect membrane potential or R_i in responsive or nonresponsive cells (R_i control, 1.3 ± 0.3 GΩ; R_i BSA, 1.3 ± 0.4 GΩ). Four of the seven responsive cells survived the transition to voltage clamp, and, in all cases, we observed T-currents (Fig. 7*D*); both nonresponsive cells survived and displayed only HVA currents.

To confirm that the sensitizing effects of reducing agents and chelators are dependent on modulation of $Ca_v3.2$, we examined the effects of these agents on the excitability of C-type nociceptors from $Ca_v3.2^{-/-}$ mice. APs were recorded from nine small, acutely dissociated $Ca_v3.2^{-/-}$ neurons. Cells had an average diameter of 24 ± 1 μm and RMPs of −65 ± 2 mV. APs had long durations (7 ± 1 ms), positive peaks (50 ± 3 mV), and long-lasting AHPs (all cells >75 ms), again consistent with identification as C-type nociceptors (Fig. 7*F*). No passive membrane properties or AP parameters were significantly different from wild-type cells with the exception of AP peaks, which were more positive ($p < 0.05$). BSA did not significantly affect threshold (Fig. 7*G*) or the probability of AP firing elicited by trains of subthreshold current injections in $Ca_v3.2^{-/-}$ cells (Fig. 7*H*,*J*). Control threshold was 1.75 ± 0.15 and 1.76 ± 0.14 nA in the presence of BSA (Fig. 7*G*). AP firing from subthreshold levels was also unaffected by L-cys, DTPA, or TPEN (Fig. 7*J*). Seven of the nine $Ca_v3.2^{-/-}$ cells survived the transition to voltage clamp, and only HVA currents were present (Fig. 7*I*). BSA did not effect membrane potential or R_i in $Ca_v3.2^{-/-}$ cells (R_i control, 1.0 ± 0.2 GΩ; R_i BSA, 1.0 ± 0.2 GΩ).

Last, we examined the ability of reducing agents to sensitize peripheral nociceptors from wild-type and $Ca_v3.2^{-/-}$ mice *in*

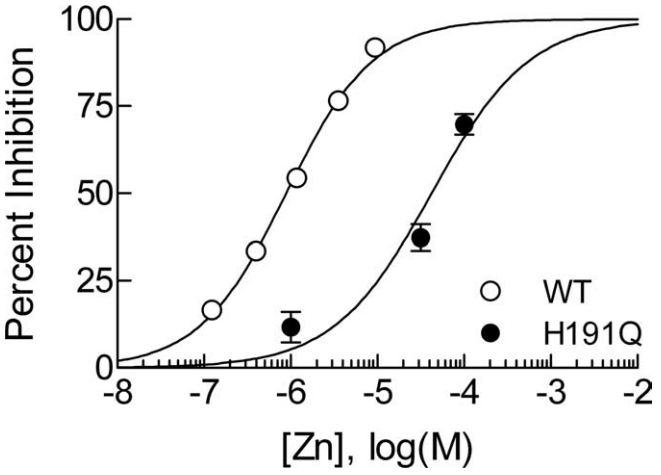

Figure 5. $Ca_v3.2$(H191Q) has reduced sensitivity to Zn^{2+}. Concentration–response curve for inhibition of $Ca_v3.2$ and $Ca_v3.2$(H191Q) by Zn^{2+} in HEK293 cells. Fitted values for IC_{50} and Hill–Langmuir coefficient (*h*) are as follows: $Ca_v3.2$, IC_{50} of 0.89 ± 0.05 μM, $h = 0.87 \pm 0.04$, $n = 4–8$; $Ca_v3.2$(H191Q), IC_{50} of 42 ± 7 μM, $h = 0.77 \pm 0.15$, $n = 4–8$. $Ca_v3.2$ data were obtained in the presence of 10 mM tricine to establish a nominally Zn^{2+}-free baseline, as well as to buffer free Zn^{2+} concentrations (see Materials and Methods). $Ca_v3.2$(H191Q) data were obtained without tricine because this channel is insensitive to chelators (Fig. 4), rendering Zn^{2+} buffering irrelevant. WT, Wild type.

vivo, by examining the effects of L-cys on PWLs from a radiant thermal stimulus. As reported previously (Choi et al., 2007) and shown in Figure 8, $Ca_v3.2^{-/-}$ mice have similar baseline PWLs to their wild-type littermate counterparts. However, wild-type littermates showed profound thermal sensitization after intradermal injection of L-cys into the ventral hindpaw at 10 and 20 min respectively, whereas $Ca_v3.2^{-/-}$ mice were unaffected (Fig. 8). Importantly, the concentration of L-cys that induced hyperalgesia in our *in vivo* experiments (100 μM) was equivalent to that which produced maximal effects on $Ca_v3.2$ currents by chelating Zn^{2+} in our *in vitro* experiments and well below the concentrations of reducing agents that have been shown to modulate other nociceptive ion channels such as TRPV1 (transient receptor potential vanilloid receptor 1) by classical redox mechanisms (Susankova et al., 2006). These results are in agreement with our previous studies examining the effects of reducing agents on peripheral nociception in rats (Todorovic et al., 2001) and confirm the absolute requirement of $Ca_v3.2$ for L-cys-evoked peripheral sensitization.

Discussion

Despite a growing body of evidence implicating T-channels in nociception (Todorovic et al., 2001; Bourinet et al., 2005; Choi et al., 2007), the cellular and molecular basis of their function in nociceptors is poorly understood. In the present study, we demonstrated that reducing agents sensitize nociceptors both *in vitro* and *in vivo* in a manner that is dependent on $Ca_v3.2$. In current-clamp experiments on acutely dissociated rat DRG neurons, we show that L-cys lowers the threshold for excitability in C-type cells that express $Ca_v3.2$ currents but not in C-type cells expressing only HVA Ca^{2+} currents. Furthermore, we show that a similar form of sensitization is present in $Ca_v3.2$ current-containing, C-type nociceptors from wild-type mice but not from $Ca_v3.2^{-/-}$ mice. Additionally, we demonstrated that reducing agents induce thermal sensitization when injected into peripheral receptive fields *in vivo*, in which putative $Ca_v3.2$ channels are located on nociceptor endings. Importantly, this sensitization is absent in

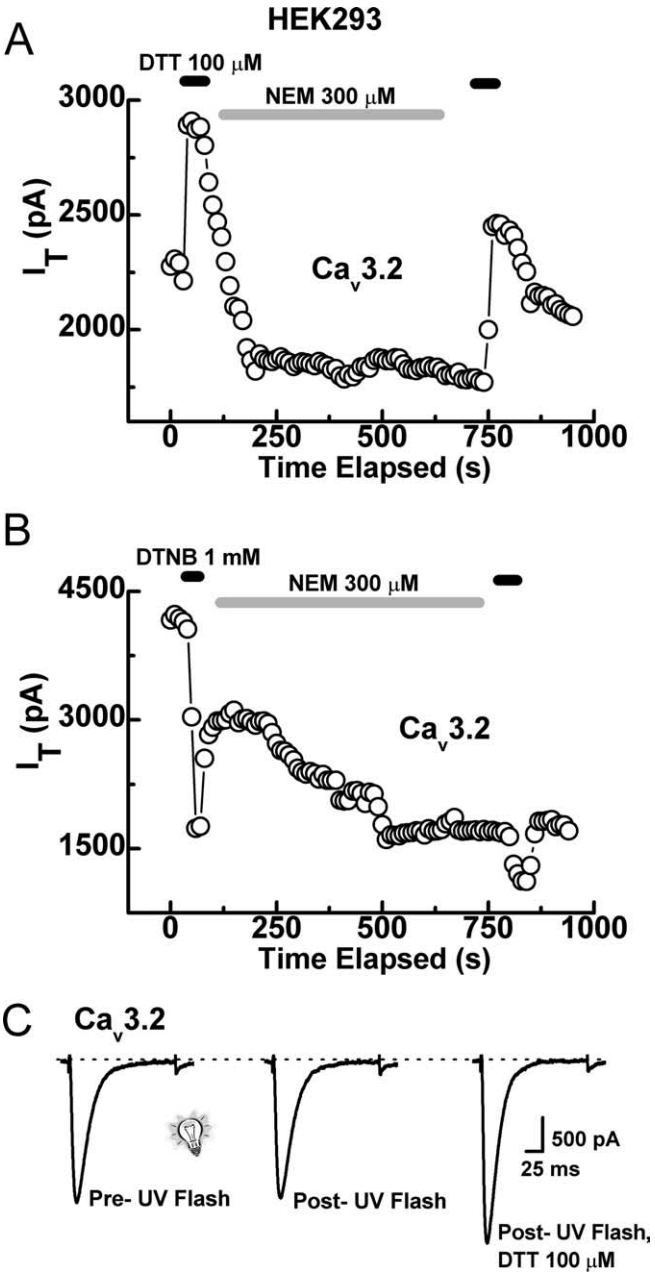

Figure 6. Cysteine-modifying agents do not disrupt the effects of reducing agents. ***A***, Time course showing that application of NEM does not disrupt the enhancement of $Ca_v3.2$ currents by DTT. For these experiments, DTT was applied first, followed by a 1–2 min wash, NEM was then applied for 8–15 min, followed by another wash, and DTT was then applied for a second time. We then compared the magnitude of the first DTT effect with that of the second (for calculation of the second effect, we considered the steady-state inhibition by NEM as a new baseline). In similar experiments from five cells, the current enhancement from the second application of DTT was 53 ± 8% compared with 45 ± 4% for the first application, indicating no inhibition of DTT by NEM. ***B***, In contrast, NEM significantly attenuated the inhibition by DTNB. The first application of DTNB produced an average inhibition of 48 ± 10% and the second only 22 ± 2% ($n = 5$; $p < 0.01$). ***C***, Representative traces showing that UV light (1 s pulse) does not modify $Ca_v3.2$ currents independently or prevent subsequent modulation by DTT. In similar experiments from four cells, DTT increased currents by 48 ± 6% after exposure to UV light.

$Ca_v3.2^{-/-}$ mice. These data suggest that, despite their modest density in C-type cells, modulation of $Ca_v3.2$ currents by endogenous agonists can influence the excitability of these nociceptors. Because C-type cells represent the majority of nociceptors, these data are helpful in understanding the contribution of T-channels

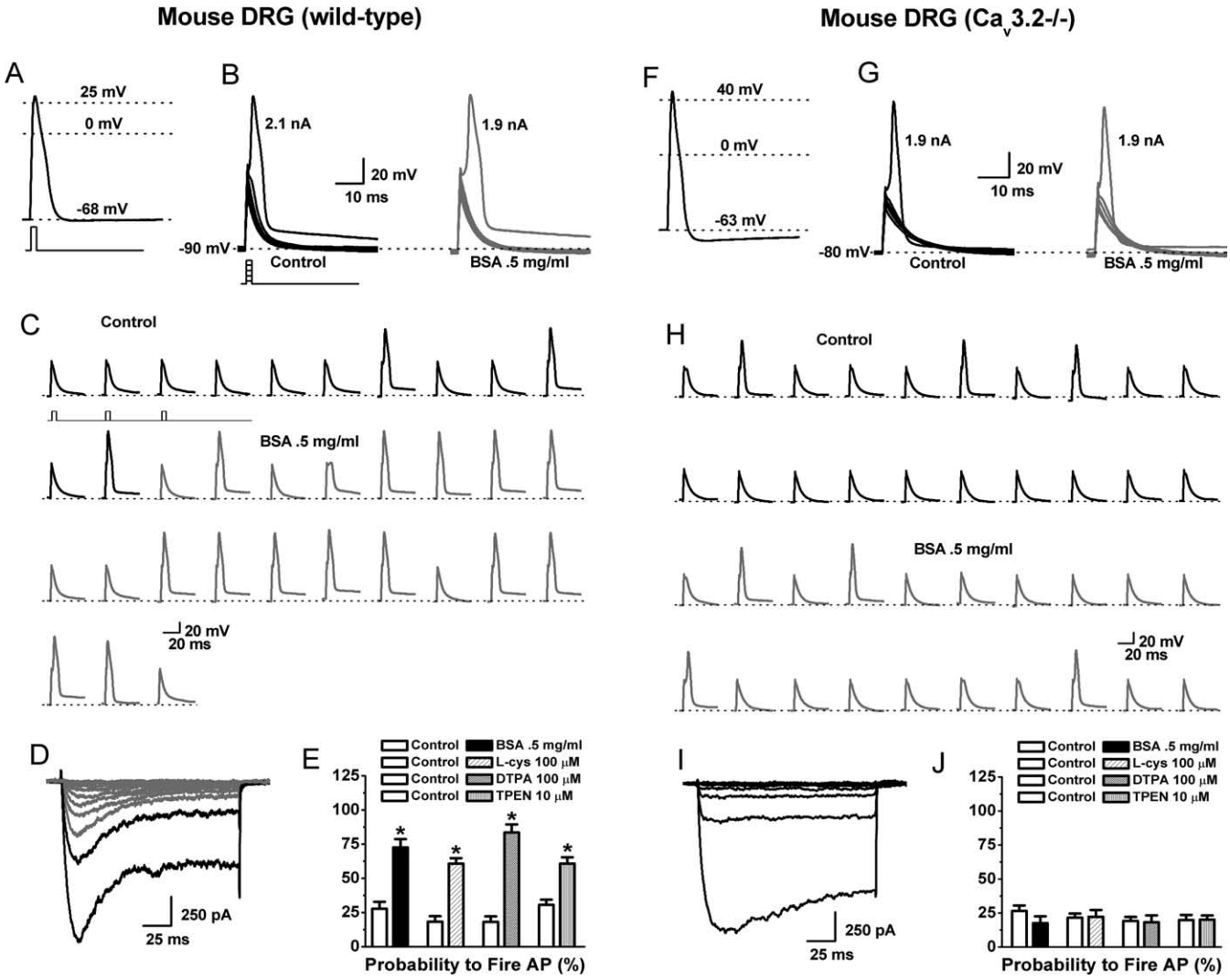

Figure 7. The effects of chelators and reducing agents on the excitability of C-type nociceptors isolated from wild-type or $Ca_v3.2^{-/-}$ mice. ***A–D*** are from a single wild-type cell; ***F–I*** are from a single $Ca_v3.2^{-/-}$ cell. ***A***, AP elicited by a 1 ms, 3 nA current injection at the RMP of the cell. ***B***, The cell was manually hyperpolarized to −90 mV and progressively greater current injections (Δ100 pA) delivered every 10 s to determine the threshold for AP firing. Threshold was 2.1 nA under control conditions (left) and 1.9 nA in the presence of BSA (right). ***C***, Continuous segment of an experiment showing that BSA increased the probability to fire APs in response to trains of subthreshold stimuli (stimuli were 1 ms, 1.9 nA delivered every 10 s). ***D***, *I–V* traces recorded in Ca^{2+} current-isolating external solution after current-clamp recording. Note the presence of both T-type (rapidly inactivating; gray lines) and HVA (slowly inactivating; black lines) currents. ***E***, Average effect of BSA, L-cys, DTPA, and TPEN on the probability to fire APs (percentage) in response to trains of subthreshold stimuli in wild-type cells (BSA: control, 27.7 ± 5.0; BSA, 72.6 ± 6.0; $p < 0.01$; L-cys: control, 18.3 ± 4.0; L-cys, 60.7 ± 4.0; $p < 0.01$; DTPA: control, 18.1 ± 4.0; DTPA, 83.5 ± 6.0; $p < 0.01$; TPEN: control, 30.6 ± 3.8; TPEN, 60.8 ± 4.6; $p < 0.01$; $n = 5–9$). ***F***, AP elicited from a $Ca_v3.2^{-/-}$ cell by a 1 ms, 3 nA current injection at the RMP cell. ***G***, Threshold was unaffected by application of BSA. ***H***, Continuous segment of an experiment showing that BSA has little effect on the probability to fire APs in response to trains of subthreshold stimuli (stimuli were 1 ms, 1.8 nA delivered every 10 s). ***I***, *I–V* traces; note the presence of only HVA currents. ***J***, Average effect of BSA, L-cys, DTPA, and TPEN on the probability to fire APs (percentage) in response to trains of subthreshold stimuli in $Ca_v3.2^{-/-}$ cells (BSA: control, 26.5 ± 4.0; BSA, 17.6 ± 5.0; L-cys: control, 21.6 ± 3.0, L-cys, 22.2 ± 5.0; DTPA: control, 19.1 ± 3.0; DTPA, 18.2 ± 5.0; TPEN: control, 19.9 ± 3.7; TPEN, 20.2 ± 3.0; $n = 7–8$).

to pain processing and may provide additional explanation for the profound effects of T-channel agonists and antagonists on pain *in vivo*.

Localization studies using *in situ* hybridization have shown mRNA for all three T-channel genes in the DRG, with high levels of $Ca_v3.2$, followed by modest levels of $Ca_v3.3$, and small levels of $Ca_v3.1$ (Talley et al., 1999). However, subsequent studies using $Ca_v3.2$ knock-out mice documented a complete loss of T-currents in small DRG neurons (Chen et al., 2003), suggesting that $Ca_v3.2$ is overwhelmingly the predominant T-channel functionally expressed in DRG nociceptors (this finding is confirmed by the present study). Additionally, we previously demonstrated that DTT and L-cys are selective for $Ca_v3.2$ currents over other T-currents, as well as other voltage- and ligand-gated currents in DRG nociceptors (Todorovic et al., 2001; Joksovic et al., 2006). Together, these findings suggest that identification of the molecular site of action of reducing agents on $Ca_v3.2$ is tantamount to identification of their site of action in DRG nociceptors.

Using chimeras constructed between $Ca_v3.1$ and $Ca_v3.2$, we were able to track the site of reducing agent modulation to domain I of $Ca_v3.2$. The sensitivity of the chimeras to DTT and L-cys mimicked their previously described inhibition by Ni^{2+} (Kang et al., 2006). Furthermore, these authors showed that mutation of a single histidine residue at position 191 severely attenuated the Ni^{2+} sensitivity of $Ca_v3.2$. This is of interest because divalent transition metals such as Cu^{2+}, Ni^{2+}, and Zn^{2+} (Jeong et al., 2003; Traboulsie et al., 2007) as well as reducing agents (Joksovic et al., 2006) are among the few pharmacological agents shown to

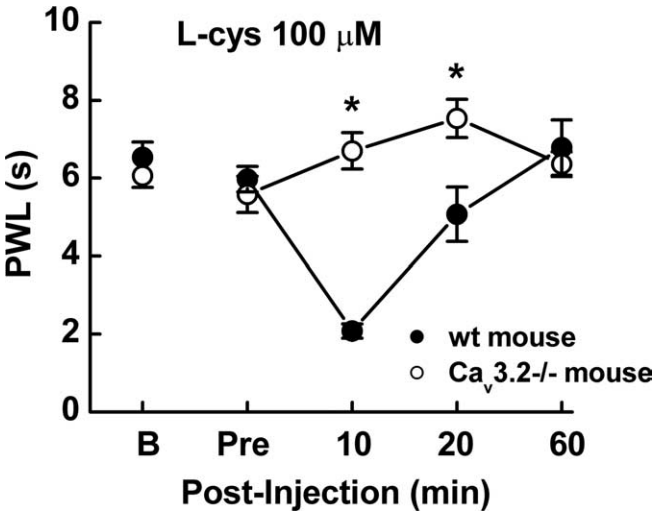

Figure 8. L-cys induces thermal hyperalgesia in wild-type but not $Ca_v3.2^{-/-}$ mice *in vivo*. L-cys induced a decrease in PWL in response to low-intensity infrared radiation (IR30) in wild-type (wt; littermate) mice but not in $Ca_v3.2^{-/-}$ mice. L-cys significantly decreased PWL at both 10 and 20 min after injection ($n = 10$; $*p < 0.05$). Wild-type PWLs reverted to baseline by 60 min after injection. "B" shows baseline PWL obtained 1 d before test; "Pre" shows the value obtained immediately before injection.

be selective for $Ca_v3.2$ over other T-currents. Similar to Ni^{2+}, we found that the H191Q mutation completely abolished the reducing agent sensitivity of $Ca_v3.2$. The basic biophysical properties of $Ca_v3.2$(H191Q) are very similar to $Ca_v3.2$, suggesting that the mutation affects modulation by reducing agents but not basic channel gating. This is further supported by the fact that the analogous reverse mutation [$Ca_v3.1$(Q172H)] was able to confer reducing agent sensitivity to the previously insensitive $Ca_v3.1$ and that inhibition by the nonselective T-channel antagonist mibefradil was similar between $Ca_v3.1$, $Ca_v3.2$, $Ca_v3.1$(Q172H), and $Ca_v3.2$(H191Q).

In addition to their abilities as cysteine modifiers, reducing agents are also excellent metal chelators, and, in general, their effects on ion channels are mediated through one or both of these mechanisms. Here, we have shown that a variety of synthetic and endogenous chelators mimic and occlude the effects of reducing agents on $Ca_v3.2$, that cysteine-modifying agents do little to disrupt the effects of DTT and L-cys on $Ca_v3.2$, and that the effects of DTT and L-cys on $Ca_v3.2$ are readily reversible. Together, our findings support the hypothesis that H191 is a critical component of an extracellular, high-affinity metal binding site on $Ca_v3.2$ and that the effects of DTT and L-cys are mediated through chelation of metals bound at this location, not through cysteine reduction. Although novel among DRG nociceptors, a similar mechanism of sensitization has been described in the heart in which lactic acid relieves a tonic Ca^{2+} block of ASICs, resulting in sensitization of the neurons that sense ischemic cardiac pain (Immke and McCleskey, 2001).

Previous studies have shown that divalent metal ions modulate T-channels by both low-affinity, voltage-dependent block and high-affinity, voltage-independent inhibition, suggesting the existence of at least two distinct metal binding sites. The low-affinity, voltage-dependent block is present in all T-channels and is likely mediated by residues in the pore-forming domains. Conversely, high-affinity, voltage-independent inhibition is present only in $Ca_v3.2$, indicating the existence of an additional, high-affinity, binding site that is unique to $Ca_v3.2$ (Lee et al., 1999; Traboulsie et al., 2007). Our data are in good agreement with these studies and support the hypothesis that H191 is a critical component of the high-affinity binding site.

The affinity of any single amino acid residue for metal ions is relatively low, which prevents free metals from binding indiscriminately to proteins. Thus, proteinaceous metal binding sites are invariably composed of two or more residues structurally coordinated to form a binding domain (Regan, 1993). Thus, it seems very likely that H191 is only one component of a larger, high-affinity metal binding site located on the external surface of $Ca_v3.2$. Furthermore, the reducing agent sensitivity of $Ca_v3.1$(Q172H) suggests that many of the residues that comprise the remainder of the site are conserved between $Ca_v3.1$ and $Ca_v3.2$. There are numerous extracellular histidine and cysteine residues conserved in domain I of T-channels that are attractive candidates for participation in metal binding, but several aspartate and glutamate residues are also possibilities. Additionally, the possibility that some components of the binding site might be located in completely separate domains from H191 must also be considered. Although distant in the amino acid sequence, these residues may come into proximity to H191 when the channel assumes its three-dimensional structure. In either case, the near total conservation of candidate residues across T-channel isoforms means that extensive mutagenesis will likely be required to elucidate the complete molecular composition of the high-affinity site.

In ion channels such as NMDA and GABA channels and ASICs in which metal chelation is an important part of the modulation by reducing agents, the metal in question is invariably Zn^{2+} (Paoletti et al., 1997; Choi and Lipton, 1999; Chu et al., 2004). Similarly, our data suggests that Zn^{2+} is the predominant metal bound to $Ca_v3.2$ in our system. However, the fact that the previously reported IC_{50} values for Cu^{2+}, Ni^{2+}, and Zn^{2+} inhibition of $Ca_v3.2$ are very similar and that $Ca_v3.2$(H191Q) has reduced sensitivity to both Ni^{2+} and Zn^{2+} suggests that the H191 site is capable of binding a variety of metals and that the identity of the metal bound will primarily depend on availability *in vitro* or *in vivo*. Cu^{2+} and Zn^{2+} are vital nutrients *in vivo* and are found in high quantities in several areas of the brain that also express $Ca_v3.2$, such as the hippocampus (Mathie et al., 2006). Thus, it is possible that one or both of these ions may modulate neuronal function via interaction with $Ca_v3.2$ under physiological or pathological conditions. Ni^{2+} is comparatively much more toxic than Cu^{2+} or Zn^{2+} and is found in much lower concentrations *in vivo* (Valko et al., 2005). Thus, although Ni^{2+} has value as a pharmacological tool *in vitro*, it is unlikely to have much significance *in vivo*.

With respect to $Ca_v3.2$ in peripheral pain pathways, Zn^{2+} seems to be the most physiologically relevant ion. Several studies have reported the existence of "zinergic" populations of DRG neurons, including C-type nociceptors (Larson and Kitto, 1997; Velazquez et al., 1999; Danscher et al., 2001). Zn^{2+} is also found in very high concentrations in the epidermis (Richelle et al., 2006) in which putative $Ca_v3.2$-containing nociceptive nerve endings are embedded. Behavioral studies also suggest that modulation of Zn^{2+} in the pain pathway can influence nociception. In studies on mice, intrathecal Zn^{2+} injections produced analgesia, whereas injection of Zn^{2+} chelators produced hyperalgesia (Larson and Kitto, 1997). When injected locally or systemically, Zn^{2+} relieves thermal hyperalgesia attributable to sciatic nerve injury in rats (Liu et al., 1999). Peripheral sensitization of C-fibers has also been documented in chronically Zn^{2+}-deficient rats (Izumi et al., 1995) as well as human patients whose plasma Zn^{2+} levels

are lowered by repeated hemodialysis (Gilchrest et al., 1982; Stahle-Backdahl, 1989).

Collectively, our data suggests that Zn^{2+} tonically inhibits $Ca_v3.2$ channels in C-type nociceptors by binding to a high-affinity site of which H191 is a critical component and that relief of this inhibition results in the enhancement of $Ca_v3.2$ currents and nociceptor sensitization. Because many nociceptors are polymodal, this mechanism of sensitization may be relevant to a variety of pain conditions involving exposure to noxious thermal, mechanical, and chemical stimuli. Furthermore, the identification of molecular mechanisms contributing to sensitization may offer insights into opportunities for analgesic pharmacotherapy.

References

Bhave G, Gereau IV RW (2004) Posttranslational mechanisms of peripheral sensitization. J Neurobiol 61:88–106.

Bourinet E, Alloui A, Monteil A, Barrere C, Couette B, Poirot O, Pages A, McRory J, Snutch TP, Eschalier A, Nargeot J (2005) Silencing of the Cav3.2 T-type calcium channel gene in sensory neurons demonstrates its major role in nociception. EMBO J 24:315–324.

Campbell JN, Meyer RA (2006) Mechanisms of neuropathic pain. Neuron 52:77–92.

Cardenas CG, Del Mar LP, Scroggs RS (1995) Variation in serotonergic inhibition of calcium channel currents in four types of rat sensory neurons differentiated by membrane properties. J Neurophysiol 74:1870–1879.

Chen CC, Lamping KG, Nuno DW, Barresi R, Prouty SJ, Lavoie JL, Cribbs LL, England SK, Sigmund CD, Weiss RM, Williamson RA, Hill JA, Campbell KP (2003) Abnormal coronary function in mice deficient in alpha1H T-type Ca^{2+} channels. Science 302:1416–1418.

Choi S, Na HS, Kim J, Lee J, Lee S, Kim D, Park J, Chen CC, Campbell KP, Shin HS (2007) Attenuated pain responses in mice lacking Ca3.2 T-type channels. Genes Brain Behav 6:425–431.

Choi Y, Chen HV, Lipton SA (2001) Three pairs of cysteine residues mediate both redox and zn^{2+} modulation of the nmda receptor. J Neurosci 21:392–400.

Choi YB, Lipton SA (1999) Identification and mechanism of action of two histidine residues underlying high-affinity Zn^{2+} inhibition of the NMDA receptor. Neuron 23:171–180.

Chu XP, Wemmie JA, Wang WZ, Zhu XM, Saugstad JA, Price MP, Simon RP, Xiong ZG (2004) Subunit-dependent high-affinity zinc inhibition of acid-sensing ion channels. J Neurosci 24:8678–8689.

Chu XP, Close N, Saugstad JA, Xiong ZG (2006) ASIC1a-specific modulation of acid-sensing ion channels in mouse cortical neurons by redox reagents. J Neurosci 26:5329–5339.

Danscher G, Jo SM, Varea E, Wang Z, Cole TB, Schroder HD (2001) Inhibitory zinc-enriched terminals in mouse spinal cord. Neuroscience 105:941–947.

Fang X, McMullan S, Lawson SN, Djouhri L (2005) Electrophysiological differences between nociceptive and non-nociceptive dorsal root ganglion neurones in the rat in vivo. J Physiol (Lond) 565:927–943.

Fayyazuddin A, Villarroel A, Le Goff A, Lerma J, Neyton J (2000) Four residues of the extracellular N-terminal domain of the NR2A subunit control high-affinity Zn^{2+} binding to NMDA receptors. Neuron 25:683–694.

Gilchrest BA, Stern RS, Steinman TI, Brown RS, Arndt KA, Anderson WW (1982) Clinical features of pruritus among patients undergoing maintenance hemodialysis. Arch Dermatol 118:154–156.

Hargreaves K, Dubner R, Brown F, Flores C, Joris J (1988) A new and sensitive method for measuring thermal nociception in cutaneous hyperalgesia. Pain 32:77–88.

Harper AA, Lawson SN (1985) Conduction velocity is related to morphological cell type in rat dorsal root ganglion neurones. J Physiol (Lond) 359:31–46.

Immke DC, McCleskey EW (2001) Lactate enhances the acid-sensing Na^+ channel on ischemia-sensing neurons. Nat Neurosci 4:869–870.

Iresjo BM, Korner U, Larsson B, Henriksson BA, Lundholm K (2006) Appearance of individual amino acid concentrations in arterial blood during steady-state infusions of different amino acid formulations to ICU patients in support of whole-body protein metabolism. JPEN J Parenter Enteral Nutr 30:277–285.

Izumi H, Mori H, Uchiyama T, Kuwazuru S, Ozima Y, Nakamura I, Taguchi S (1995) Sensitization of nociceptive C-fibers in zinc-deficient rats. Am J Physiol 268:R1423–R1428.

Jeong SW, Park BG, Park JY, Lee JW, Lee JH (2003) Divalent metals differentially block cloned T-type calcium channels. NeuroReport 14:1537–1540.

Jevtovic-Todorovic V, Wozniak DF, Powell S, Nardi A, Olney JW (1998) Clonidine potentiates the neuropathic pain-relieving action of MK-801 while preventing its neurotoxic and hyperactivity side effects. Brain Res 781:202–211.

Joksovic PM, Nelson MT, Jevtovic-Todorovic V, Patel MK, Perez-Reyes E, Campbell KP, Chen CC, Todorovic SM (2006) CaV3.2 is the major molecular substrate for redox regulation of T-type Ca^{2+} channels in the rat and mouse thalamus. J Physiol (Lond) 574:415–430.

Kang HW, Park JY, Jeong SW, Kim JA, Moon HJ, Perez-Reyes E, Lee JH (2006) A molecular determinant of nickel inhibition in Cav3.2 T-type calcium channels. J Biol Chem 281:4823–4830.

Krezel A, Lesniak W, Jezowska-Bojczuk M, Mlynarz P, Brasun J, Kozlowski H, Bal W (2001) Coordination of heavy metals by dithiothreitol, a commonly used thiol group protectant. J Inorg Biochem 84:77–88.

Larson AA, Kitto KF (1997) Manipulations of zinc in the spinal cord, by intrathecal injection of zinc chloride, disodium-calcium-EDTA, or dipicolinic acid, alter nociceptive activity in mice. J Pharmacol Exp Ther 282:1319–1325.

Lee JH, Gomora JC, Cribbs LL, Perez-Reyes E (1999) Nickel block of three cloned T-type calcium channels: low concentrations selectively block alpha1H. Biophys J 77:3034–3042.

Leszkiewicz D, Aizenman E (2002) A role for the redox site in the modulation of the NMDA receptor by light. J Physiol (Lond) 545:435–440.

Leszkiewicz DN, Aizenman E (2003) Reversible modulation of GABA(A) receptor-mediated currents by light is dependent on the redox state of the receptor. Eur J Neurosci 17:2077–2083.

Li C, Peoples RW, Weight FF (1996) Proton potentiation of ATP-gated ion channel responses to ATP and Zn^{2+} in rat nodose ganglion neurons. J Neurophysiol 76:3048–3058.

Liu T, Walker JS, Tracey DJ (1999) Zinc alleviates thermal hyperalgesia due to partial nerve injury. NeuroReport 10:1619–1623.

Mathie A, Sutton GL, Clarke CE, Veale EL (2006) Zinc and copper: Pharmacological probes and endogenous modulators of neuronal excitability. Pharmacol Ther 111:567–583.

Nelson MT, Joksovic PM, Perez-Reyes E, Todorovic SM (2005) The endogenous redox agent L-cysteine induces T-type Ca^{2+} channel-dependent sensitization of a novel subpopulation of rat peripheral nociceptors. J Neurosci 25:8766–8775.

Pan ZH, Zhang X, Lipton SA (2000) Redox modulation of recombinant human GABA(A) receptors. Neuroscience 98:333–338.

Paoletti P, Ascher P, Neyton J (1997) High-affinity zinc inhibition of NMDA NR1-NR2A receptors. J Neurosci 17:5711–5725.

Perez-Reyes E, Cribbs LL, Daud A, Lacerda AE, Barclay J, Williamson MP, Fox M, Rees M, Lee JH (1998) Molecular characterization of a neuronal low-voltage-activated T-type calcium channel. Nature 391:896–900.

Petruska JC, Napaporn J, Johnson RD, Gu JG, Cooper BY (2000) Subclassified acutely dissociated cells of rat DRG: Histochemistry and patterns of capsaicin-, proton-, and ATP-activated currents. J Neurophysiol 84:2365–2379.

Regan L (1993) The design of metal-binding sites in proteins. Annu Rev Biophys Biomol Struct 22:257–287.

Richelle M, Sabatier M, Steiling H, Williamson G (2006) Skin bioavailability of dietary vitamin E, carotenoids, polyphenols, vitamin C, zinc and selenium. Br J Nutr 96:227–238.

Scroggs RS, Fox AP (1992) Calcium current variation between acutely isolated adult rat dorsal root ganglion neurons of different size. J Physiol (Lond) 445:639–658.

Stahle-Backdahl M (1989) Uremic pruritus. clinical and experimental studies. Acta Derm Venereol Suppl (Stockh) 145:1–38.

Sullivan JM, Traynelis SF, Chen HS, Escobar W, Heinemann SF, Lipton SA (1994) Identification of two cysteine residues that are required for redox modulation of the NMDA subtype of glutamate receptor. Neuron 13:929–936.

Sundberg RJ, Martin BR (1974) Interactions of histidine and other imidazole derivatives with transition metal ions in chemical and biological systems. Chem Rev 74:471–517.

Susankova K, Tousova K, Vyklicky L, Teisinger J, Vlachova V (2006) Reduc-

ing and oxidizing agents sensitize heat-activated vanilloid receptor (TRPV1) current. Mol Pharmacol 70:383–394.

Talley EM, Cribbs LL, Lee JH, Daud A, Perez-Reyes E, Bayliss DA (1999) Differential distribution of three members of a gene family encoding low voltage-activated (T-type) calcium channels. J Neurosci 19:1895–1911.

Thio LL, Zhang HX (2006) Modulation of inhibitory glycine receptors in cultured embryonic mouse hippocampal neurons by zinc, thiol containing redox agents and carnosine. Neuroscience 139:1315–1327.

Todorovic SM, Jevtovic-Todorovic V, Meyenburg A, Mennerick S, Perez-Reyes E, Romano C, Olney JW, Zorumski CF (2001) Redox modulation of T-type calcium channels in rat peripheral nociceptors. Neuron 31:75–85.

Traboulsie A, Chemin J, Chevalier M, Quignard JF, Nargeot J, Lory P (2007) Subunit-specific modulation of T-type calcium channels by zinc. J Physiol (Lond) 578:159–171.

Valko M, Morris H, Cronin MT (2005) Metals, toxicity and oxidative stress. Curr Med Chem 12:1161–1208.

Velazquez RA, Cai Y, Shi Q, Larson AA (1999) The distribution of zinc selenite and expression of metallothionein-III mRNA in the spinal cord and dorsal root ganglia of the rat suggest a role for zinc in sensory transmission. J Neurosci 19:2288–2300.

Vitko I, Chen Y, Arias JM, Shen Y, Wu XR, Perez-Reyes E (2005) Functional characterization and neuronal modeling of the effects of childhood absence epilepsy variants of CACNA1H, a T-type calcium channel. J Neurosci 25:4844–4855.

Welsby PJ, Wang H, Wolfe JT, Colbran RJ, Johnson ML, Barrett PQ (2003) A mechanism for the direct regulation of T-type calcium channels by Ca^{2+}/calmodulin-dependent kinase II. J Neurosci 23:10116–10121.

Wilkins ME, Smart TG (2002) Redox modulation of GABAA receptors obscured by Zn^{2+} complexation. Neuropharmacology 43:938–944.